

Exact Results for Interacting Hard Rigid Rotors on a d -Dimensional Lattice

Sushant Saryal^{1,*} and Deepak Dhar^{1,†}

¹*Department of Physics, Indian Institute of Science Education and Research, Pune 411008, India*

(Dated: February 22, 2022)

We study the entropy of a set of identical hard objects, of general shape, with each object pivoted on the vertices of a d -dimensional regular lattice of lattice spacing a , but can have arbitrary orientations. When the pivoting point is situated asymmetrically on the object, we show that there is a range of lattice spacings a , where in any orientation, a particle can overlap with at most one of its neighbors. In this range, the entropy of the system of particles can be expressed exactly in terms of the grand partition function of coverings of the base lattice by dimers at a finite negative activity. The exact entropy in this range is fully determined by the second virial coefficient. Calculation of the partition function is also shown to be reducible to that of the same model with discretized orientations. We determine the exact functional form of the probability distribution function of orientations at a site. This depends on the density of dimers for the given activity in the dimer problem, that we determine by summing the corresponding Mayer series numerically. These results are verified by numerical simulations.

Many organic liquids, on cooling, first freeze into a state where there is long range crystalline order, but the molecules are partly able to rotate about their center of mass. In contrast to the liquid crystals that shows orientational order, but no positional order, these materials show no long range orientational order, and have been called plastic solids, rotator crystals or orientationally disordered solids. Timmermans studied it in the 1930's², and early work has been summarized in³. These are currently attracting a lot of interest, for applications such as storage batteries⁴, drug delivery⁵, and refrigeration⁶.

The simplest theoretical description of this state would be to assume that rigid molecules have their centers of mass fixed at lattice positions, but have orientational degrees of freedom. Many such models have been studied since the beginning of these studies, e.g.⁷. Casey and Runnels⁸ studied a system of hard squares with centers fixed on the one dimensional lattice and also with centers free to move along a 1D line. Freasier and Runnels⁹ studied a model of rotors with their centers pivoted on a one dimensional lattice. More recently, Kantor and Kardar¹⁰, and Gurin and Varga¹¹ studied a system of hard rods in isobaric ensemble with their centers restricted to move only along a 1D line but free to rotate in a plane. In an earlier paper, we have studied hard linear rods, with centers fixed on sites of a 1-d lattice, but free to rotate in a plane¹². We showed that even in one dimension, this system shows an infinite number of singularities of entropy per rod as a function of the ratio of length of rods and the lattice spacing. Plastic solids often show many (three or more) crystalline phases with varying amount of orientational order¹³. It is gratifying that the simple model of rigid hard particles can describe this basic phenomenology.

There are few exact results available for this problem in more than one dimension. In this work, we show that in this model of rigid rotors on a lattice [an example in two dimensions is shown in Fig. 1], there is a range of lattice spacings in which the model becomes reducible to the dimer model on the same lattice with a negative value

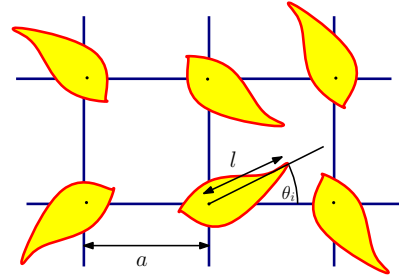


FIG. 1. An example of hard particles with their pivots fixed at sites of a square lattice of lattice spacing a . The farthest point in the object from the pivot is at distance ℓ . The orientation of the rotor at site \mathbf{i} is specified by the orientation of the long axis to the x -axis θ_i .

of the dimer activity. We determine the exact functional form of the probability distribution function of orientations at a site. This depends on the density of dimers for the given activity in the dimer problem, that we determine by summing the corresponding Mayer series numerically. These results are valid for general shapes of rotors, and for arbitrary lattices, and dimensions. We have verified these results by numerical simulations for thin hard linear rods pivoted at one end at the vertices of a square lattice [Fig. 2].

One important feature of the model is the fact that interaction between two rotors has a different form in different directions. In some cases, e.g. in the class of models known as compass models¹⁴, this feature leads to the model becoming analytically tractable. The best known example of this class is the Kitaev model¹⁵. In the standard version of the Kitaev model, the degrees of freedom are quantum spins, though the classical case has also been studied¹⁶. We will only study the case of classical rotors here.

We consider a system of hard bodies, called rotors, of identical shape and size in d dimensions. Each rotor has a marked point called the pivot, which is at the same

relative position in each rotor. The objects are rigid, of a given shape. Our treatment is valid for arbitrary shapes. The pivots of the particles are fixed at the vertices of a regular d -dimensional lattice (e.g. the d -dimensional hypercubical lattice), but the rotors can take arbitrary orientations, subject to the constraint that different rotors cannot overlap. The orientation of the rotor at the vertex \mathbf{r} of the lattice may be specified by a $d \times d$ real orthogonal matrix $M(\mathbf{r})$. Then, the full configuration is specified by a lattice model, with a $d \times d$ matrix belonging to the group $SO(d)$ at each vertex. [Sometimes, the experimentally prepared crystals are racemic mixtures of the two species of molecules related by mirror symmetry. These crystals would be described by the group $O(d)$. Our treatment is easily extended to this case.]

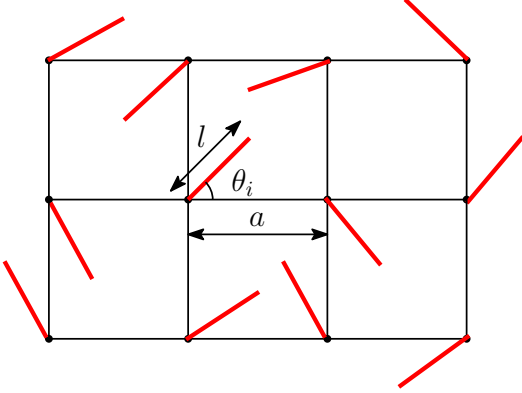


FIG. 2. Hard rods pivoted at the one end on a square lattice. Length of each rod is l , lattice spacing is a . The orientation of rotor at site \mathbf{i} is given by the angle its long axis makes with the x-axis.

We first consider the case when the pivot is placed asymmetrically on the rotor, and there is a unique point on the rotor at maximum distance from the pivot. Let this distance be denoted by ℓ . Let the distance between nearest neighbors vertices of the lattice be a . The line joining the pivot to the farthest point will be called the long axis of the rotor. Then, we will study the entropy per site for this model, as a function of the dimensionless coupling parameter ℓ/a , for a specified shape of the object.

We define the indicator function $\eta(\mathbf{a}, \mathbf{b})$ to be 1 if the rotors at sites \mathbf{a} and \mathbf{b} , with given orientations $M(\mathbf{a})$ and $M(\mathbf{b})$, overlap, and zero otherwise. For notational simplicity, we will not show the dependence on orientations explicitly. Then the partition function for this system is defined as

$$\mathcal{Z}_N = \left[\prod_{\mathbf{r}} \int dM(\mathbf{r}) \right] \prod_{\langle \mathbf{a}, \mathbf{b} \rangle} [1 - \eta(\mathbf{a}, \mathbf{b})], \quad (1)$$

where the second product is over all nearest neighbor pairs, and the integral over the matrix $M(\mathbf{r})$ is the normalized Haar measure over the group $SO(d)$, so that $\int dM(\mathbf{r}) 1 = 1$. We will only consider the case where

rotors at sites farther than nearest neighbors cannot overlap, and second product is restricted to only over nearest neighbor pairs. The entropy per site $s(\ell/a)$ is defined by

$$s(\ell/a) = \lim_{N \rightarrow \infty} [\log Z_N]/N, \quad (2)$$

where N is the number of sites in the lattice. If $\ell/a < 1/2$, then different rotors cannot overlap, and the entropy per rotor takes its maximum value, zero in our normalization. As the spacing a is decreased, keeping ℓ constant, the entropy will also decrease. When a is decreased to the minimum allowed value, corresponding to closest packing, entropy per rotor will tend to $-\infty$.

Now consider the case $\ell/a = 1/2 + \epsilon$, where ϵ is a small positive number. Consider two rotors at nearest neighbor vertices \mathbf{i} and \mathbf{j} along the bond along one of the lattice directions, say $\hat{\mathbf{e}}_1$. Then, these two rotors can overlap only if the long axes of both are substantially aligned parallel to the direction $\hat{\mathbf{e}}_1$. We define ω_1 as set of orientations of the rotor at \mathbf{i} such that there is a non-empty set of orientations of the rotor at \mathbf{j} that overlap with the rotor at \mathbf{i} . The volume of the set ω_1 decreases to zero, as ϵ tends to zero.

We similarly construct sets $\omega_{-1}, \omega_{\pm 2}, \dots, \omega_{\pm d}$, using other neighbors of \mathbf{i} (set $\omega_{-\alpha}$ corresponds to the $-\hat{\mathbf{e}}_\alpha$ direction). The total number of such sets is the number of neighbors of \mathbf{i} , i.e. $2d$ on the d -dimensional hypercubical lattice. For small ϵ , these sets ω_i are disjoint. As a is decreased, the sets ω_i 's increase in size, and eventually, some will touch. Let a^* be the smallest value of a such that the sets ω_i are still disjoint. Then for all the range of values $2\ell > a > a^*$, a rotor at any site \mathbf{i} , in any orientation $M(\mathbf{i})$ can have an overlap with at most one of its neighbors, whatever their orientations. Let \mathbf{j} and \mathbf{j}' be two neighbors of \mathbf{i} , with $\mathbf{j} \neq \mathbf{j}'$. Then we have, for all $\mathbf{i}, \mathbf{j}, \mathbf{j}'$, and all orientations $M(\mathbf{i}), M(\mathbf{j}), M(\mathbf{j}')$,

$$\eta(\mathbf{i}, \mathbf{j})\eta(\mathbf{i}, \mathbf{j}') = 0. \quad (3)$$

We will call this the at-most-one-overlap (AOO) condition.

A simple example of systems where AOO condition holds in some region of the parameter space is hard rigid lines of length ℓ , where one of the ends is the pivoting point as shown in Fig. 2. In this case, it is straightforward to verify that $a^* = \sqrt{2}\ell$, and determine explicitly the function $\eta(\theta, \theta')$. The details are given in Appendix A.

Now, we expand the product in Eq. (1), and make a graphical representation of the terms of the expansion, with a bond between vertices \mathbf{i} and \mathbf{j} , iff the term contains $\eta(\mathbf{i}, \mathbf{j})$, see Fig. 3. This is a lattice version of the well-known *Mayer cluster expansion*. Then, using the AOO condition, only graphs with at most one bond coming to a site survive. Thus, we get

$$\mathcal{Z}_N = \mathcal{Z}_{\text{dimers}}(z), \quad (4)$$

where $\mathcal{Z}_{\text{dimers}}(z)$ is the grand partition function of partial covering of the vertices of the lattice by dimers (see

Fig. 3),

$$\mathcal{Z}_{\text{dimers}}(z) = \sum_{\text{dimer-configs}} z^{\text{number of dimers}}, \quad (5)$$

with the fugacity of a dimer is the (negative) real number, given by

$$z = - \int dM(\mathbf{i}) \int dM(\mathbf{j}) \eta(\mathbf{i}, \mathbf{j}). \quad (6)$$

In fact, z is exactly the second virial coefficient B_2 of the virial expansion. It is straight forward to determine it for a given shape of molecules. In Fig. 4, we have plotted z as a function of ℓ/a for the case of linear rods, pivoted at one end shown in Fig. 2. Let $g(z)$ be the logarithm of the grand partition function per site, defined as

$$g(z) = \lim_{N \rightarrow \infty} [\log \mathcal{Z}_{\text{dimers}}(z)]/N \quad (7)$$

Then, the entropy per site is $s(\ell/a) = g(z)$.

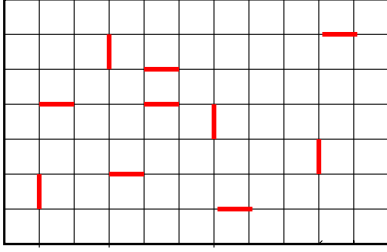


FIG. 3. A typical term in the graphical expansion of the partition function [Eq.(1)]. This can also be thought of as a configuration of a set of dimers on the lattice.

The evaluation of the partition function of partial covering of dimers is a well-known hard problem in lattice statistics, and no exact expression for $g(z)$ is known, except in one dimension and in some special graphs, like the Bethe lattice. However, the equivalence is not without use, as we see that the exact entropy $s(\ell/a)$, in the entire range of a satisfying the AOO condition, depends on shape of the rotors, only through the second virial coefficient z .

Also, we note that the equality of the dimer and rotor model partition functions holds also for finite lattices of size $L_1 \times L_2 \times L_3 \dots$. The dependence of these partition functions on one of the dimensions is of the form

$$\mathcal{Z} \sim \sum_{\alpha} c_{\alpha} \lambda_{\alpha}^{L_1}, \quad (8)$$

where λ_{α} are the eigenvalues of the transfer matrix in the direction 1, and c_{α} are some constants. Since this is true for all L_1 , we conclude that *all* the nonzero eigenvalues of the transfer matrix for the rotor model are the same as eigenvalues of the transfer matrix for the dimer model with activity z . In Appendix B and C, we show an explicit calculation of the model for hard rods on a

line and zigzag lattice respectively, using transfer matrices, and show that the results agree with the algebraic method used here.

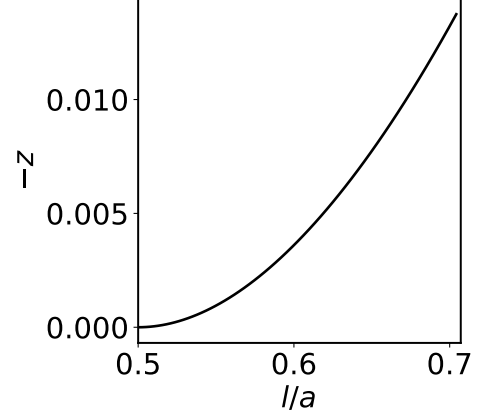


FIG. 4. $-z$ vs l/a , for a system of hard linear rods of length l pivoted at one end on 2d square lattice.

We will now show that under the AOO condition, our model with continuous $SO(d)$ degrees of freedom is reducible to a discrete model with $2d$ discrete degrees of freedom per site. Following the terminology of ice and KDP models¹⁷, we will call this model the Hydrogen Iodide (HI) model, where the heavy “iodine”(I) atoms sit at lattice sites, and there is one “hydrogen”(H) atom near each I atom that sits along one of the nearest neighbor bonds, close to it. There is a repulsive energy cost if the H atoms of two adjacent I’s sit on the same bond. Thus, there is a discrete degree of freedom at each site \mathbf{r} of the lattice, denoted by $\sigma(\mathbf{r})$, which takes *non-zero* integer values between $-d$ and d . If the hydrogen atom is along the bond $\hat{\mathbf{e}}_{\alpha}$, we will call the state α , if along $-\hat{\mathbf{e}}_{\alpha}$, we call the state $-\alpha$ ($1 \leq \alpha \leq d$). Therefore, for a bond between the sites \mathbf{i} and $\mathbf{i} + \hat{\mathbf{e}}_{\alpha}$, the energy cost is J iff the spin at site \mathbf{i} is in the state α , and that at site $(\mathbf{i} + \hat{\mathbf{e}}_{\alpha})$ is in the state $-\alpha$. The interaction along the bond in the direction $\hat{\mathbf{e}}_{\alpha}$ only involves the spin states $\pm\alpha$.

The hamiltonian of the model is

$$\mathcal{H}_{HI} = J \sum_{\mathbf{r}} \sum_{\alpha=1}^d \delta(\sigma(\mathbf{r}), \alpha) \delta(\sigma(\mathbf{r} + \hat{\mathbf{e}}_{\alpha}), -\alpha), \quad (9)$$

where $\delta(a, b)$ is the Kronecker delta function. We write $\exp[-\beta J \delta(a, b)] = 1 + \tilde{z} \delta(a, b)$, with $\tilde{z} = e^{-\beta J} - 1$, β is the inverse temperature, and expand the partition function in powers of \tilde{z} , we again get the partition functions of dimers with activity $z = \tilde{z}/(2d)^2$. Let Z_{HI} denote the partition function of the HI model, then we have,

$$Z_{HI} = (2d)^N \mathcal{Z}_{\text{dimers}}\left(z = \frac{\tilde{z}}{(2d)^2}\right) \quad (10)$$

To complete the correspondence with the rotors models, we break the manifold of states given by M into

$2d$ equal submanifolds. A given matrix M is associated with the discrete state α of the HI model as follows: we imagine starting with a large value of the lattice spacing a , and decreasing it slowly, and monitor the overlap integral with neighbour in the direction α , for fixed M . At some value of spacings, one of the integrals becomes non zero for the first time. That is the direction of the HI model spin associated to this M . Values on M which lie at the common boundaries of two submanifolds, and where this direction is not unique, have zero measure. For all smaller a , this overlap will increase, but by definition, all other overlaps will remain strictly zero, so long as the AOO condition is satisfied. As a simple example, in two dimensions, the manifold M is the full circle with $0 \leq \theta \leq 2\pi$, and it is broken into four submanifolds $([-\pi/4, \pi/4], [\pi/4, 3\pi/4], [3\pi/4, 5\pi/4])$ and $[5\pi/4, 7\pi/4])$ which correspond to the four states of the discrete model.

The graphical expansion of the partition function, for a given dimer configuration, the sites covered by dimers have a fixed σ -variable, and we sum over all orientations of arrows at sites where there is no dimer. The full partition function has the form of the inclusion-exclusion principle. The empty dimer configuration corresponds to all possible states of the discrete spins. The term with one dimer is negative, and subtracts the sum of contributions where specified one bond is doubly occupied, and others are arbitrary, summed over all possible positions of the bond. The next term corrects for the overcounting by adding the contribution where two bonds are doubly occupied, and others are arbitrary, and so on. Then the integration over submanifolds for specified discrete state at each site is easily done. In the integration over the M -variables, restricted to specific submanifolds, sites not covered by same dimer are independent. This implies that all the n -point correlation functions of rotor model with AOO condition can be expressed as linear functions of the n -point correlations of \mathcal{H}_{HI} . We illustrate this below using the 1-point function.

Let $f_\alpha(M)dM$ be the conditional probability that variable M of the rotor at \mathbf{O} lies in a small volume dM near the value M , given that it overlaps with the neighboring rotor in the direction α .

Then we have

$$f_\alpha(M) = \frac{\int dM(\hat{\mathbf{e}}_\alpha) \eta(\mathbf{O}, \hat{\mathbf{e}}_\alpha)}{\int dM(\mathbf{O}) \int dM(\hat{\mathbf{e}}_\alpha) \eta(\mathbf{O}, \hat{\mathbf{e}}_\alpha)}, \quad (11)$$

In Fig. 5, we have shown the plot of $f_1(\theta)$ for the linear rods pivoted at the end. Clearly f_α is zero outside the the submanifold ω_α .

Let $P(M)dM$ denote the probability that the matrix at the origin \mathbf{O} , in the thermodynamical limit, lies in the volume dM centered at M . In the partition sum in Eq.(1), we sum over all sites, except the origin. If $\bar{n}(z)$ is the number density of dimers per site, then with probability weight $(1 - 2\bar{n}(z))$, the site is not covered by a dimer, and with weight $\frac{\bar{n}(z)}{d}$, it is covered by a dimer in

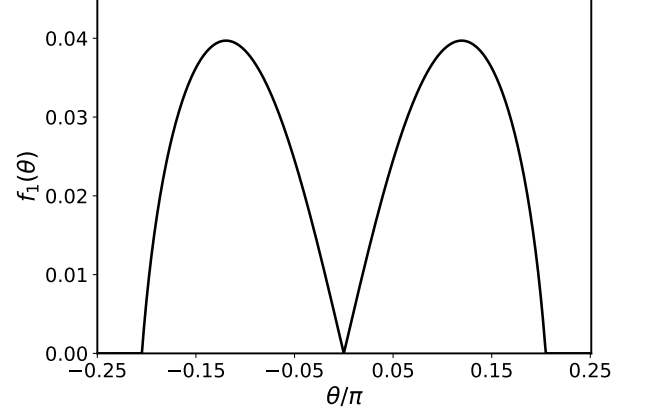


FIG. 5. $f_1(\theta)$ for a system of hard linear rods of length $2d$ square lattice for $a = 1.6l$. Because of the symmetry of the square lattice other f_α are related to f_1 such that $f_{-1}(\theta) = f_1(\theta - \pi)$ and $f_{\pm 2}(\theta) = f_1(\theta \pm \pi/2)$.

direction α . Then $P(M)$ is given by,

$$P(M) = \left[(1 - 2\bar{n}) + \frac{\bar{n}}{d} \sum_{\alpha} f_{\alpha}(M) \right]. \quad (12)$$

As a concrete example, we calculate $P(M)$ for thin hard linear rods of length ℓ pivoted at one end at the vertices of a square lattice [Fig. 2]. Here M is just a simple rotation angle $\theta \in [-\pi, \pi)$. In this case, it is straight forward to calculate the function $f_\alpha(\theta)$, for $\alpha = \pm 1, \pm 2$, numerically for any given value of ℓ/a using Eq.(11).

In Fig. 6, we have plotted the function $P(\theta)$, as determined by Monte Carlo simulations, against the theoretical form, for different values of ℓ/a . We do not have the functional form of $\bar{n}(z)$, as the solution to the dimer model is not known. However, the experimental data can be fitted to the functional form in Eq.(12), treating the unknown value $\bar{n}(z)$ as a single fitting parameter, for a given value of ℓ/a . This is done in Fig. 6, and we see that using only a single parameter, we are able to get a very good fit to the function $P(\theta)$ for the entire range of θ , and for different values of ℓ/a . In Appendix B and C, we verify that the distribution of orientations also agrees with that calculated using the eigenvectors of the transfer matrix for the 1-dimensional chain, and the zig-zag chain.

In Fig. 7, we have plotted the fitting value of $\bar{n}(z)$ as a function of the overlap integral z for different values of ℓ/a . As already mentioned, exact functional form of $\bar{n}(z)$ is not known. But, for the low values of activity in the range where AOO holds, it is adequate to use first few terms in the low density Mayer series for the dimer

density as a function of the activity z :

$$\bar{n}(z) = \sum_{n=1}^{\infty} (-1)^{n-1} a_n z^n \quad (13)$$

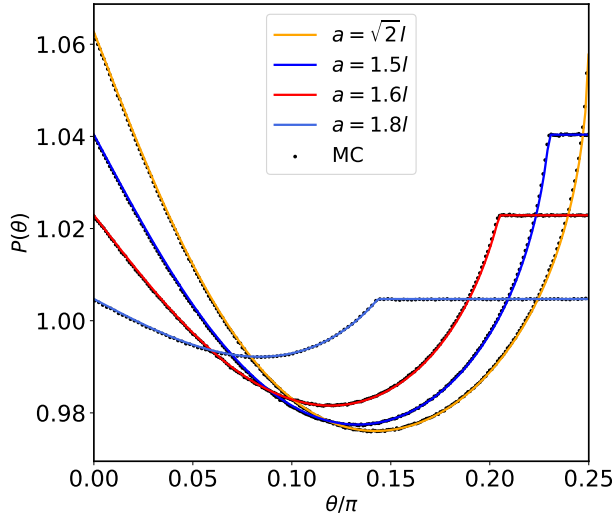


FIG. 6. The probability distribution of angles $P(\theta)$ as a function of the orientation angle θ , for a system of hard rods pivoted at the one end on a square lattice (see Fig. 2), for different values of lattice spacing. The function outside this range can be obtained using the symmetries of the square lattice.

It was shown by Viennot that the Mayer coefficients a_n are integers equal to the number of heaps one can form on the simple cubic lattice using dimers¹⁸. For small values of z of interest here, only the first few terms of this series are enough to determine $\bar{n}(z)$ to three digit accuracy, which is given by

$$\bar{n}(z) = 2 [z - 7z^2 + 58z^3 - 521z^4 \dots] \quad (14)$$

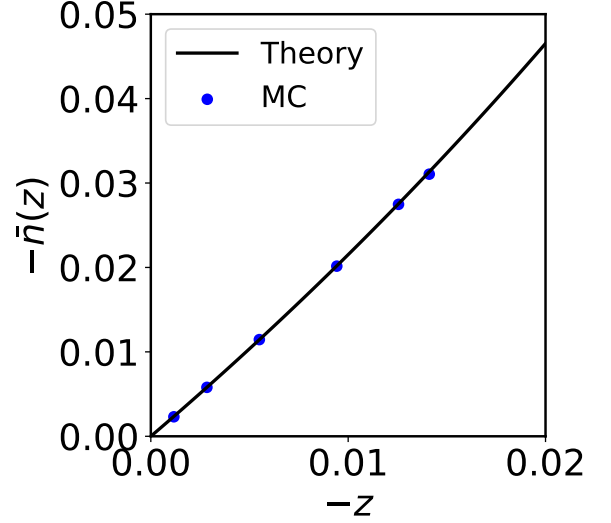


FIG. 7. Plot of negative of average density $\bar{n}(z)$ per site obtained from Monte Carlo simulations and theoretical value given by eq.(14).

At $\ell/a = 1/\sqrt{2}$, the value of activity is approximately $z = -0.014$, which is much less than the radius of convergence of the series in Eq.(14). Even though the value of z is rather small, the effect on $P(\theta)$ is quite substantial as is seen in Fig. 6. From the listed few terms above, we can estimate that the radius of convergence is near 0.1 (a much more precise estimate is clearly possible, but this is adequate for our purpose here). This can be understood as follows: We need the AOO condition to establish the equivalence between the rotors model and the dimer model. The breakdown of the AOO condition is due to geometrical reasons specific to the rotors model. The dimer model partition function shows no singularity as a function of activity, if the lattice spacing is decreased so that the AOO condition is no longer satisfied.

Of course, the rotors model is well defined, even outside the range of lattice parameters where the AOO condition is satisfied, the minimum lattice spacing allowed being set by density of closest packing. The mechanism leading to geometrical transitions discussed in¹² is quite robust, and holds in all dimensions. If we decrease a below a^* , we would expect to get a sequence of geometrical transitions. In addition, there can be other order-disorder type of transitions.

As a is decreased below $a^* = \sqrt{2}l$, the function $z(a)$ is a smooth function of a , but there are configurations there one dimer overlaps with two others. These give rise to non-zero positive correction to the entropy $s(\ell/a)$. If $a = a^*(1 - \epsilon)$, this correction is of order $\epsilon^{3/2}$ (see Appendix D).

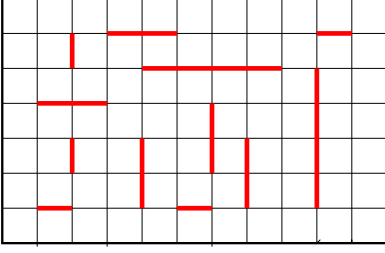


FIG. 8. A typical term in the graphical expansion of the partition function of rotors, when the objects are reflection symmetric, and the AOO condition is not satisfied. Here, the terms can be thought of as configurations in the grand partition function of a system of polydisperse straight rods on the lattice, where the activity of a rod depends on its length.

Now, we discuss the case where the pivot point is a center of inversion of the rotor. For example, the two-dimensional case, when rotors are elliptical, with pivot at the center of the ellipse. In this case, AOO condition can not be satisfied on the square lattice, but there is a range of values of a , such that an ellipse can touch two other ellipses, only if the centers are collinear. Then, the graphical representation, terms that contribute can be thought of as configurations of non-overlapping straight needles, whose length can be any integer. The weight of a needle depends on its length (see Fig. 8). Thus, in this case, the partition function becomes equivalent to that of a polydisperse long rods on the same lattice. The latter problem has been studied numerically, but remains quite intractable analytically.

As a final remark we want to point out that this analysis is also valid for soft rods. In case of attractive interaction among rods z will be positive.

In summary, we have shown that there is a range of lattice spacings, where the calculation of partition function of the rotor model becomes exactly equivalent to the problem of evaluating the dimer model partition function on the same lattice, analytically continued to negative activities of dimers. This equivalence allows us to determine the distribution of orientations for the original model. The results agree with direct Monte Carlo simulation of the rotor model. The results are valid for arbitrary shapes of molecules, and all dimensions.

It is hoped that insights from the rather idealized model will help generate a better understanding of the actual plastic crystals.

Acknowledgments: We thank M. Barma, K. Damle, J. Klamser, S. N. Majumdar, R. Rajesh, T. Sadhu, and G. J. Sreejith for their comments on the paper. DD's work is supported by a Senior Scientist fellowship from the National Academy of Sciences of India. S.S. acknowledges financial support from Council of Scientific and Industrial Research (Grant No. 1061651988).

APPENDIX A: CALCULATION OF $\eta(\theta, \theta')$ FOR THIN HARD LINEAR RODS PIVOTED AT ONE END

Consider two thin hard rods of length l placed at adjacent sites, see Fig. 9. $\eta(\theta, \theta')$ will be 1 when they overlap and 0 otherwise, see Fig. 10. For notational convenience we define $\kappa = l/a$. Then, if $\kappa < 1/2$, each rod can rotate fully freely, and $\eta(\theta, \theta') = 0$ for all θ, θ' .

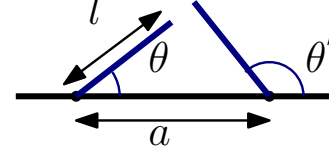


FIG. 9. Two thin hard rods pivoted at adjacent lattice sites.

While AOO condition in 2d square lattice is valid for $1/2 \leq \kappa \leq 1/\sqrt{2}$, for 1d case, which we will discuss in next section, it is valid for $1/2 \leq \kappa \leq 1$. Therefore, we will discuss here the full range $1/2 \leq \kappa \leq 1$. Because of the symmetry of the problem we have $\eta(\theta, \theta') = \eta(-\theta, -\theta')$, we will only consider $\theta > 0$ to determine $\eta(\theta, \theta')$.

For $1/2 \leq \kappa \leq 1/\sqrt{2}$, there is no overlap if $|\theta| > \cos^{-1}(\frac{1}{2\kappa})$. If $0 < \theta < \cos^{-1}(\frac{1}{2\kappa})$ rods will overlap only if $\theta' \in [\theta'_{min}, \theta'_{max}]$ where

$$\theta'_{max} = \pi + \theta - \sin^{-1} \left[\frac{\sin \theta}{\kappa} \right] \quad (A1)$$

$$\theta'_{min} = \pi - \tan^{-1} \left[\frac{\kappa \sin \theta}{1 - \kappa \cos \theta} \right] \quad (A2)$$

For $1/\sqrt{2} \leq \kappa \leq 1$, there is no overlap if $|\theta| > \sin^{-1}(\kappa)$. Here θ'_{max} has the same expression as given in eq.(A1) but θ'_{min} has different expression for two different ranges of θ . For $\theta \in [\cos^{-1}(\frac{1}{2\kappa}), \sin^{-1}(\kappa)]$

$$\theta'_{min} = \theta + \sin^{-1} \left[\frac{\sin \theta}{\kappa} \right] \quad (A3)$$

For $0 < \theta < \cos^{-1}(\frac{1}{2\kappa})$ θ'_{max} is given by eq.(A1). A graphical representation of $\eta(\theta, \theta')$ is given in Fig. 10, for some representative values of l/a .

Given the functional form of $\eta(\theta, \theta')$, the integral in equation (6) of main text is easily done numerically, to determine z as a function of l/a .

APPENDIX B: TRANSFER MATRIX CALCULATION FOR THE 1-DIMENSIONAL CHAIN OF HARD THIN RODS PIVOTED AT ONE END

We consider a system of thin hard rigid linear rods, each of length l . One end of the rods is fixed on regular

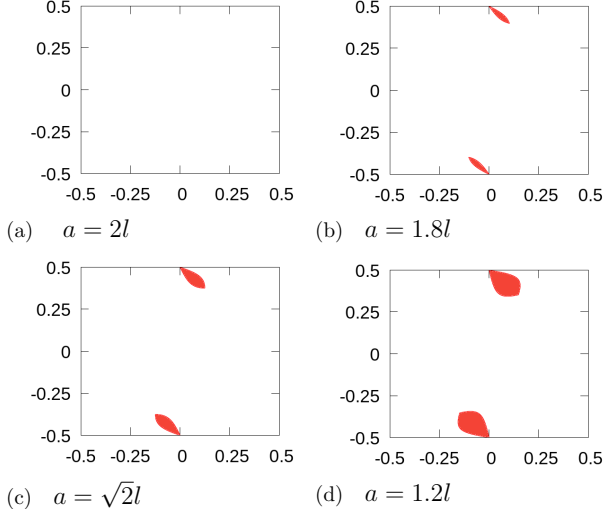


FIG. 10. $\eta(\theta, \theta')$ in $(\frac{\theta}{2\pi}, \frac{\theta'}{2\pi})$ plane. Shaded area (red) corresponds to overlap region where η is 1. In the unshaded area $\eta = 0$.

lattice of spacing a , and the rods can rotate in a plane, see Fig. 11. The orientation of each rod is specified by the angle it makes with the x-axis. Let the angle the i th rod makes be called θ_i , with $-\pi \leq \theta_i < \pi$.

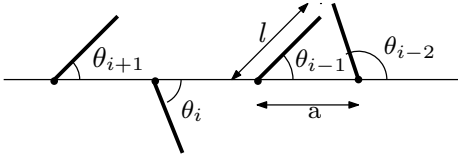


FIG. 11. A system of hard rods pivoted at one end on a one dimensional lattice.

Then we partition function is given by,

$$\mathcal{Z}_L = \left[\prod_i \int \frac{d\theta_i}{2\pi} \right] \prod_{i=1}^{L-1} [1 - \eta(\theta_{i+1}, \theta_i)] \quad (\text{B1})$$

We will obtain the entropy per rod using the transfer matrix method, which provides a check of the algebraic method used in the main text. Also, we can obtain the probability distribution of the angles $P(\theta)$ in terms of the eigenvector of the transfer matrix, which also agrees with the result obtained in the main text.

AOO condition is clearly satisfied if $1/2 \leq \kappa \leq 1$. Let $\mathcal{Z}_L(\theta)$ be the restricted partition function of the system of L hard rods with left most rod having angle θ . Then it satisfies the following recursion relation

$$\mathcal{Z}_{L+1}(\theta) = \int_{-\pi}^{\pi} \frac{d\theta'}{2\pi} \mathcal{T}(\theta, \theta') \mathcal{Z}_L(\theta') \quad (\text{B2})$$

where \mathcal{T} is the transfer matrix. It is 0 when the adjacent rods with angles (θ, θ') overlap and 1 when they don't overlap see Fig. 10. Then the free energy per site in the thermodynamic limit is given by $\log(\lambda)$ where λ is the largest eigenvalue of the transfer matrix \mathcal{T}_κ , whose eigenequation is given by

$$\int \frac{d\theta'}{2\pi} \mathcal{T}(\theta, \theta') \psi_\lambda^R(\theta') = \lambda \psi_\lambda^R(\theta) \quad (\text{B3})$$

where $\psi_\lambda^R(\theta)$ is the right eigenfunction of integral kernel $\mathcal{T}(\theta, \theta')$. Clearly

$$\mathcal{T}(\theta, \theta') = 1 - \eta(\theta, \theta'). \quad (\text{B4})$$

Now, $\eta(\theta, \theta')$ is nonzero only if $\cos \theta > 0$, and $\cos \theta' < 0$. Thus, we see that the AOO condition is satisfied

$$\eta(\theta, \theta') \eta(\theta', \theta'') = 0, \text{ for all } \theta, \theta', \theta'', \quad (\text{B5})$$

Let us define function $f(\theta)$ given by

$$f(\theta) = \int \frac{d\theta'}{2\pi} \eta(\theta, \theta'). \quad (\text{B6})$$

Clearly, $f(\theta)$ is nonzero only if, $|\theta| < \cos^{-1}(\frac{1}{2\kappa})$ for $1/2 \leq \kappa \leq \sqrt{2}$ and $|\theta| < \sin^{-1}(\kappa)$ for $1/\sqrt{2} \leq \kappa \leq 1$, and it equals to $[\theta'_{\max}(\theta) - \theta'_{\min}(\theta)]/(2\pi)$. Then it is easily seen that the right eigenfunction is given by

$$\psi_\lambda^R(\theta) = 1 - \frac{1}{\lambda} f(\theta), \quad (\text{B7})$$

where eigenvalue λ satisfies the equation

$$\lambda^2 - \lambda + A = 0 \quad (\text{B8})$$

where A is the fraction area of the forbidden region (red region in Fig. 10), given by

$$A = \int \frac{d\theta}{2\pi} \int \frac{d\theta'}{2\pi} \eta(\theta, \theta'). \quad (\text{B9})$$

Thus the larger eigenvalue is given by

$$\lambda = \frac{1 + \sqrt{1 - 4A}}{2} \quad (\text{B10})$$

Now it is easily that for dimer model in one dimension with activity z , eigenvalue of the transfer matrix is given by,

$$\lambda_{\text{dimers}} = \frac{1 + \sqrt{1 + 4z}}{2} \quad (\text{B11})$$

Hence the model of hard rods is equivalent to the dimer model provided $z = -A$.

In order to obtain the probability distribution $P(\theta)$ we need both left and right eigenfunctions of the transfer

matrix. Because of the symmetry of the problem left eigenfunction is simply, $\psi_\lambda^L(\theta) = \psi_\lambda^R(\theta - \pi)$. Then $P(\theta)$ is given by (see Fig. 12)

$$P(\theta) = \frac{1 - \frac{1}{\lambda}[f(\theta) + f(\theta - \pi)]}{1 + \frac{2}{\lambda}z}. \quad (\text{B12})$$

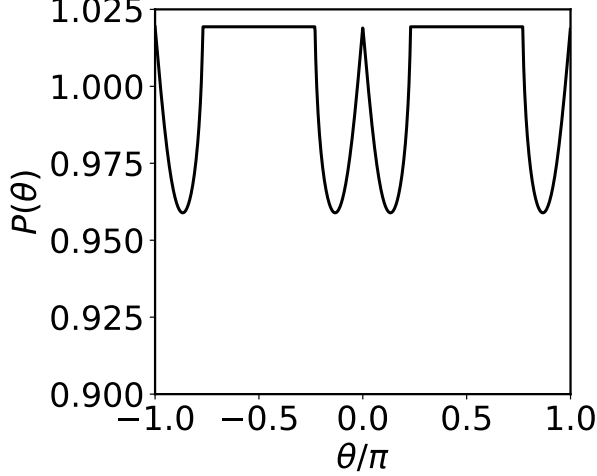


FIG. 12. Probability distribution of angles for 1-dimensional chain of hard thin rods pivoted at one end. $a = 1.5l$.

APPENDIX C: TRANSFER MATRIX FOR THE ZIGZAG CHAIN

We consider a slightly more complicated case of a one-dimensional zigzag lattice, where the angle between adjacent bonds alternates between two values ϕ and $-\phi$ [Fig. 13]. At each site is a linear rigid thin rod of length ℓ pivoted to lattice site at its midpoint. The orientation of the rod at site i will be specified with its angle θ_i it makes with one of the bond directions. We can choose the angle to lie in the range $[-\pi/2, +\pi/2]$.

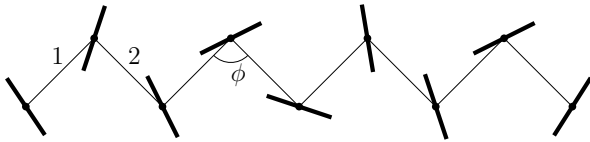


FIG. 13. System of hard rods pivoted at center on a 1-dimensional zigzag lattice. Type 1 and Type 2 bonds make $(\pi/2 - \phi/2)$ and $(-\pi/2 + \phi/2)$ angles from the x-axis respectively.

Each rod is free to rotate about its center as long as it do not overlap with other rods.

In this case, in the transfer matrix method, we get two coupled eigenvalue equations of the form

$$\mathcal{T}_1 |g\rangle = \lambda |f\rangle \quad (\text{C1})$$

$$\mathcal{T}_2 |f\rangle = \lambda |g\rangle \quad (\text{C2})$$

Here \mathcal{T}_1 and \mathcal{T}_2 are the transfer matrices along the two alternating bonds. We write \mathcal{T}_1 and \mathcal{T}_2 as

$$\mathcal{T}_1 = |1\rangle \langle 1| - \Delta_1 \quad (\text{C3})$$

$$\mathcal{T}_2 = |1\rangle \langle 1| - \Delta_2 \quad (\text{C4})$$

where $|1\rangle$ is a vector whose value in θ representation is always one and $\Delta_{1,2}$ is the overlap operator which in θ representation takes value 1 when there is a overlap between adjacent rods and takes value zero otherwise. In this case, the AOO condition becomes

$$\Delta_1 \Delta_2 = \Delta_2 \Delta_1 = 0. \quad (\text{C5})$$

Then the following vectors are solutions of eq.(C1) and eq.(C2)

$$|f\rangle = (1 - \frac{1}{\lambda} \Delta_2) |1\rangle \quad (\text{C6})$$

$$|g\rangle = (1 - \frac{1}{\lambda} \Delta_1) |1\rangle \quad (\text{C7})$$

where the eigenvalue λ satisfies following quadratic equation

$$\lambda^2 - \lambda + A = 0 \quad (\text{C8})$$

where A is , as before, given by

$$\begin{aligned} A &= \langle 1 | \Delta_1 | 1 \rangle = \langle 1 | \Delta_2 | 1 \rangle \\ &= \int_{-\pi/2}^{\pi/2} \frac{d\theta}{\pi} \int_{-\pi/2}^{\pi/2} \frac{d\theta'}{\pi} \langle \theta' | \Delta_{1,2} | \theta \rangle \end{aligned} \quad (\text{C9})$$

which is nothing but the area of the overlap region. Again we are able to obtain the same result obtained by analytic method by using simple algebraic property of the transfer matrix given by eq.(C5). In Fig. 14 colored area corresponds to the region where AOO condition is satisfied in the $(a/l, \phi)$ plane.

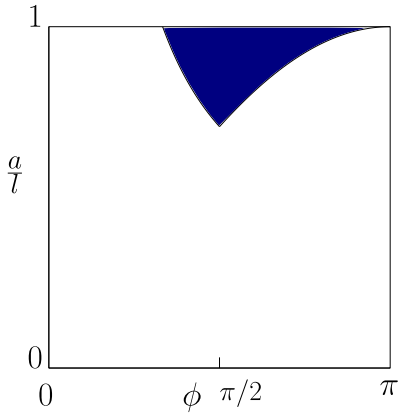


FIG. 14. Colored area corresponds the region where AOO condition is valid.

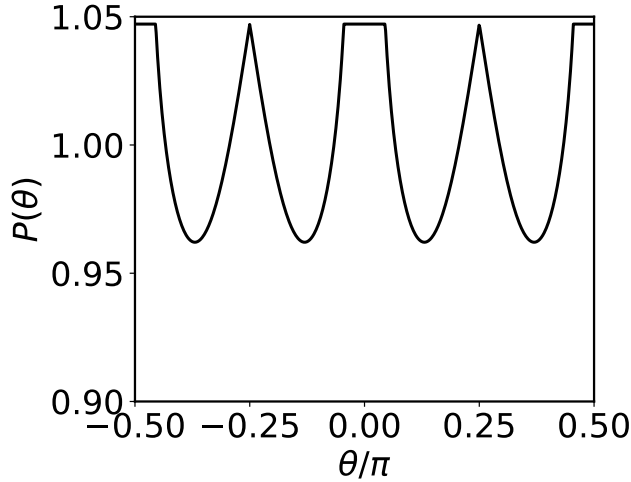


FIG. 15. Probability distribution for system of rods are pivoted at the center on a one-dimensional zigzag lattice. $a = 0.8l$ and $\phi = \pi/2$

Probability distribution $P(\theta)$ can also calculated from eigenvectors, given by (see Fig. 15),

$$P(\theta) = \frac{1 - \frac{1}{\lambda}[\langle \theta | \Delta_1 | 1 \rangle + \langle \theta | \Delta_2 | 1 \rangle]}{1 + \frac{2}{\lambda}z}. \quad (\text{C10})$$

where $z = -A$ as before.

APPENDIX D: QUALITATIVE BEHAVIOUR OF THE ENTROPY FOR LATTICE SPACING JUST BELOW a^*

In this section we will consider 2-dimensional model of hard rods pivoted at one end on lattice site (see Fig. 2 of main text), when lattice spacing $a = a^*(1 - \epsilon)$ with $\epsilon \ll 1$. We present a heuristic argument that for this case, we have

$$\begin{aligned} s(l/a) &= g(z), & a > a^* \\ &= g(z) + k\epsilon^{3/2} + \text{higher order terms in } \epsilon, & a < a^* \end{aligned} \quad (\text{D1})$$

where z is the dimer activity corresponding to lattice spacing a given by eq.(6) of main text.

If AOO condition is violated, there are configuration where one rotor overlaps with two neighbours. A typical case is shown in Fig. 16

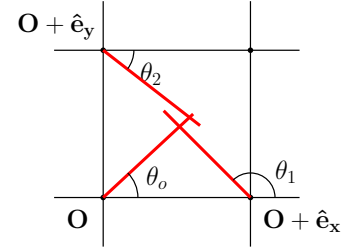


FIG. 16. Rotor at \mathbf{O} overlaps simultaneously with rotors at $\mathbf{O} + \hat{\mathbf{e}}_y$ and $\mathbf{O} + \hat{\mathbf{e}}_x$.

The contribution of such configurations to the partition function is of the form,

$$\int \frac{d\theta_o}{2\pi} \int \frac{d\theta_1}{2\pi} \int \frac{d\theta_2}{2\pi} \eta(\theta_o, \theta_1) \eta(\theta_o, \theta_2).$$

It is clear from the geometry of the figure that non-zero contribution to the integral happens only when, $(\theta_o - \pi/4)$, $(\theta_1 - 3\pi/4)$ and $(\theta_2 + \pi/4)$ must be of order $\epsilon^{1/2}$ and thus integral is of order $\epsilon^{3/2}$. This integral makes positive contribution to the partition function. Hence we get the result given in eq.(D1).

* sushant.saryal@students.iiserpune.ac.in

† deepak@iiserpune.ac.in

¹ L. Onsager, The Effects of Shape on the Interaction of Colloidal Particles, Ann. N.Y. Acad. Sci. **51**, 627 (1949).

² J. Timmermans, Plastic crystals: a historical review, J. Phys. Chem. Solids, **18** (1961), pp. 1-8.

³ L. A. K. Staveley, Thermodynamic studies of molecular

rotation in solids, J. Phys. Chem. Solids, Vol. 18, (1961) pp46-52.

⁴ Jennifer M. Pringle, Patrick C. Howlett, Douglas R. MacFarlane and Maria Forsyth, Organic ionic plastic crystals: recent advances, J. Mater. Chem., 2010, 20, 2056-2062. DOI: 10.1039/B920406G

⁵ E. Shalaev, K. Wu, S. Shamblyn, J.F. Krzyzaniak, M.

- Descamps Crystalline mesophases: structure, mobility, and pharmaceutical properties Adv. Drug Deliv. Rev., 100 (2016), pp. 194-211.
- ⁶ Li, B., Kawakita, Y., Ohira-Kawamura, S. et al. Colossal barocaloric effects in plastic crystals. Nature 567, 506–510 (2019). <https://doi.org/10.1038/s41586-019-1042-5>.
 - ⁷ J. A. Pople and F. E. Karasz, A Theory of fusion of molecular crystals: I. The effect of hindered rotation, J. Phys. Chem. Solids, **18**, (1961) pp 28-39.
 - ⁸ L. M. Casey and L. K. Runnels, Model for Correlated Molecular Rotation ,J. Chem. Phys. **51**, 5070 (1969).
 - ⁹ B. C. Freasier and L. K. Runnels , Classical rotators on a linear lattice, J. Chem. Phys. **58**, 2963 (1973).
 - ¹⁰ Y. Kantor and Mehran Kardar , One-dimensional gas of hard needles, Phys. Rev E **79**, 041109(2009).
 - ¹¹ P. Gurin and S. Varga, Towards understanding the ordering behavior of hard needles: Analytical solutions in one dimension, Phys. Rev. E **83**, 061710 (2011).
 - ¹² S. Saryal, J. U. Klamser, T. Sadhu and Deepak Dhar, Multiple Singularities of the Equilibrium Free Energy in a One-Dimensional Model of Soft Rods, Phys. Rev. Lett. **121**, 240601(2018).
 - ¹³ G. B. Guthrie and J. P McCullough, Some observations on phase transformations in molecular crystals, J. Phys. Chem. Solids, **18** pp53-61(1961).
 - ¹⁴ Zohar Nussinov, Jeroen Van Den Brink, Compass models: Theory and physical motivations, Rev. Mod. Phys., Vol. 87 (2015) pp1-59.
 - ¹⁵ Alexei Kitaev, Anyons in an exactly solvable model and beyond, Ann. Phys. Vol. 321 (2006) pp2-111.
 - ¹⁶ G. Baskaran, Diptiman Sen, and R. Shankar, Spin-S Kitaev model: Classical ground states, order from disorder, and exact correlation functions, Phys. Rev. **B 78** (2008) 115116.
 - ¹⁷ E. Lieb and Fa Yueh Wu, Two dimensional Ferroelectric models, in *Phase transitions and critical phenomena*, Vol. 1, Ed. C. Domb and M. S. Green, [Academic Press, London, 1972], pp 332-490.
 - ¹⁸ G. X. Viennot, in *Proc. of the Colloque de Combinatoire Enumerative*, Lecture Notes in Mathematics Vol. 1234, pp 321-350 (Springer-Verlag, Berlin, 1986).
 - ¹⁹ Julianne Klamser, Tridib Sadhu, and Deepak Dhar, Sequence of phase transitions in a model of interacting rods, arXiv:2202.03065.